A Theory of Capillary Rise of a Liquid in a Vertical Cylindrical Tube and in a Parallel-Plate Channel

Washburn Equation Modified to Account for the Meniscus with Slippage at the Contact Line[1]

SAMUEL LEVINE, JAMES LOWNDES, ERIC J. WATSON, AND GRAHAM NEALE

Department of Mathematics, University of Manchester, Manchester, England and Department of Chemical Engineering, University of Ottawa, Ottawa, Canada

Received May 8, 1978; accepted May 16, 1979

The classic equation of Washburn and Rideal for the rate of displacement due to surface tension forces of air by a liquid in a vertical capillary tube is based on the steady-flow parabolic velocity profile of Poiseuille across a section of the capillary. However, such a model of incompressible liquid flow cannot apply at the two ends of the liquid column in the capillary. The departure from Poiseuille flow in the vicinity of the advancing meniscus in a vertical cylindrical capillary is examined under the following assumptions. (i) The meniscus retains a fixed shape, which is the sector of a sphere making an angle of contact α with the capillary wall. (ii) The liquid has risen up the tube to reach a sufficiently slow quasi-steady flow, when both the acceleration and nonlinear inertia terms may be ignored. (iii) The usual nonslip flow condition is assumed at the tube wall except in the immediate region of the three-phase contact line, where the slip velocity is proportional to the shear stress exerted on the solid tube. The two regions are matched by the method of "inner" and "outer" expansions. (iv) At the meniscus, the tangential shear stress is zero and continuity of normal stress is approximated by assuming a fixed spherical shape. A generalization of Washburn's formula for the rate of rise of the meniscus as a function of height in a cylindrical tube is obtained. The meniscus exerts an extra drag which increases the effective height by an amount that increases with decrease in contact angle and the dimensionless ratio (slip coefficient/tube radius). A similar treatment of the flow near the meniscus moving up a parallel-plate channel is presented and a corresponding increase in drag due to the meniscus is obtained.

1. INTRODUCTION

Recently, Wingrave *et al.* (1) uncovered early papers by Lucas (2) and Bosanquet (3) on the classic equation, usually named after Washburn (4) and Rideal (5), for the rate of displacement, due to surface tension forces, of gas by a liquid in a vertical capillary tube. The paper by Lucas preceded those of Washburn and Rideal and Bosanquet introduced a correction to Rideal's equation by starting with a momentum balance. This correction was discussed by Levine *et al.* (6, 7), without referring to Bosanquet's early work. The equations of the above four early authors are based on the steady-state parabolic velocity profile of Poiseuille across a section of the capillary and, as such, cannot apply in the region of entry into the tube from a reservoir. A resulting anomaly is the impossible prediction of an initial infinite acceleration at entry. By studying the entry flow with an energy balance treatment, Szekely *et al.* (8) removed the initial infinity in the fluid motion and Levine *et al.* (7) improved their theory in a study of the sink flow toward the capillary entrance from the

[1] Presented in part at 51st National Colloid and Surface Science Meeting, American Chemical Society, Buffalo, June 1977.

0021-9797/80/010136-16$02.00/0

reservoir. The various modifications to the classic work referred to above take no account of the departure from Poiseuille flow in the vicinity of the advancing liquid/gas meniscus. The present paper deals with this deviation from Poiseuille flow in a vertical cylindrical tube and also in a vertical parallel-plate channel, under the condition that the flow up the tube or channel is well developed.

Huh and Scriven (9) and Dussan and Davis (10) have shown that the usual nonslip flow condition at a solid boundary leads to a physically impossible infinite stress exerted on the solid at the three-phase contact line where the meniscus meets the solid boundary. This anomaly of infinite stress can be removed by postulating a slip condition in the immediate vicinity of the contact line but retaining the nonslip condition at macroscopic distances from the contact line on the liquid/solid boundary. These two regions are matched by the asymptotic method of "inner" and "outer" expansions (11, 12). A number of authors have examined two-phase flow either between parallel plates or in a cylindrical tube. Bataille (13) and Bhattacharji and Savic (14) obtained solutions of the flow for a liquid–gas interface under the restriction that the interface remains planar at a contact angle of 90°. However they did not mention the anomaly of the infinite force due to the nonslip flow condition at the three-phase contact line. Huh and Mason (15) and Hocking (16) have examined the steady motion of a liquid meniscus in a capillary tube in which slippage of the liquid on the solid is permitted at the contact line. These authors only considered contact angles equal to or close to 90°. Earlier, Hansen and Toong (17) had determined numerically the outer expansion for fluid flow in a cylindrical tube at arbitrary contact angle, but omitted the inner expansion in the immediate vicinity of the contact line. From their experimental (18) and theoretical (17) work they found that for small tube radii (<1 mm) where gravity effects can be ignored, and small capillary numbers ($<10^{-3}$) (capillary number = viscosity × meniscus velocity/interfacial tension), the meniscus shape is little changed from a spherical sector, except near the contact line. This result is confirmed by Huh and Mason (15) and also by numerical solutions of the Navier–Stokes equations with the full boundary stress conditions at the liquid–gas interface which are currently being obtained by us.

The following assumptions are made here in the study of two-phase (liquid/gas) flow up a vertical cylindrical pipe of radius a. (i) The meniscus retains a fixed shape, which is the sector of a sphere making an angle α with the pipe wall. Continuity of normal stress is approximated by assuming the spherical shape. (ii) The liquid has risen up the tube to reach a (sufficiently slow) quasi-steady state, when both the acceleration and nonlinear inertia terms may be ignored. (iii) The usual nonslip flow condition holds at the pipe wall except in the immediate region of the three-phase contact line, where the anomaly of infinite stress is removed by postulating that the slip velocity is proportional to the shear stress exerted on the solid pipe. Use is made of the inner expansion obtained by Hocking (16) and of an outer expansion similar to that of Hocking (16). Similar assumptions are made with the flow model for the parallel-plate channel system.

2. FLOW CONDITIONS IN MENISCUS REGION OF CYLINDRICAL TUBE

We introduce cylindrical polar coordinates (r,θ,z) and corresponding fluid velocity components $(v,0,u)$ (Fig. 1). The origin 0 is on the axis of the tube at the entry position; z is distance upward along the vertical axis, r is measured from the axis normal to it in a horizontal plane, and θ is the angle of rotation about the axis. By symmetry the flow conditions are independent of angle θ. The velocity components v, u and the pressure p are functions of z and time t. For an in-

compressible fluid the equation of continuity is

$$\frac{\partial}{\partial r}(rv) + r\frac{\partial u}{\partial z} = 0, \qquad [2.1]$$

and the Navier–Stokes equations are

$$\frac{\partial v}{\partial t} + v\frac{\partial v}{\partial r} + u\frac{\partial v}{\partial z} = -\frac{1}{\rho}\frac{\partial p}{\partial r} + \frac{\mu}{\rho}\left(\frac{\partial^2 v}{\partial r^2} + \frac{1}{r}\frac{\partial v}{\partial r} + \frac{\partial^2 v}{\partial z^2}\right), \qquad [2.2]$$

$$\frac{\partial u}{\partial t} + u\frac{\partial u}{\partial z} + v\frac{\partial u}{\partial r} = -\frac{1}{\rho}\frac{\partial p}{\partial z} + \frac{\mu}{\rho}\left(\frac{\partial^2 u}{\partial r^2} + \frac{1}{r}\frac{\partial u}{\partial r} + \frac{\partial^2 u}{\partial z^2}\right) - g, \qquad [2.3]$$

where ρ and μ are the density and viscosity respectively of the fluid and g is the acceleration due to gravity. We shall assume that the fluid has risen up the tube to reach a sufficiently slow quasi-steady-state flow, when the nonlinear terms may also be ignored and therefore the left-hand sides of [2.2] and [2.3] can be replaced by zero. These conditions suggest as a reasonable assumption a fixed shape for the meniscus, whose height at time t is given by

$$z = h(t) + f(r), \qquad [2.4]$$

where $h(t)$ is the meniscus height on the axis of the tube and therefore $f(0) = 0$.

It is convenient to write $u = u(r,z,t)$ in the form

$$u = 2\dot{h}(t)\left(1 - \frac{r^2}{a^2}\right) + \dot{h}(t)u_0(r,z), \qquad [2.5]$$

where the first term on the right-hand side represents Poiseuille flow and $\dot{h}(t)u_0(r,z)$ is the correction which should be significant near the meniscus. For incompressible flow,

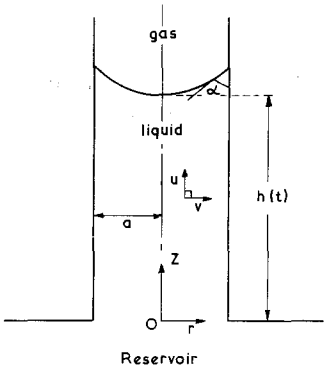

FIG. 1. The coordinate system and velocity components for flow up a cylindrical capillary tube.

in the absence of inertia terms,

$$\nabla^2 p = \frac{\partial^2 p}{\partial r^2} + \frac{1}{r}\frac{\partial p}{\partial z} + \frac{\partial^2 p}{\partial z^2} = 0. \qquad [2.6]$$

Substitution of [2.5] into [2.3] (in which the left-hand side is zero) suggests the partitioning of the pressure such that

$$p = -\left(\rho g + \frac{8\mu\dot{h}(t)}{a^2}\right)z + \dot{h}(t)p_0(r,z), \qquad [2.7]$$

and hence [2.3] and [2.6] yield

$$\frac{\partial^2 u_0}{\partial r^2} + \frac{1}{r}\frac{\partial u_0}{\partial r} + \frac{\partial^2 u_0}{\partial z^2} = \frac{1}{\mu}\frac{\partial p_0}{\partial z}, \qquad [2.8]$$

$$\frac{\partial^2 p_0}{\partial r^2} + \frac{1}{r}\frac{\partial p_0}{\partial r} + \frac{\partial^2 p_0}{\partial z^2} = 0. \qquad [2.9]$$

The first term on the right hand side of [2.7] is the pressure in Poiseuille flow. A particular solution of [2.9] which is finite at $r = 0$, can be written as

$$p_0 = \mu J_0(kr)(Ce^{-kz} + De^{kz}), \qquad [2.10]$$

where k, C, and D are complex constants and J_n is the Bessel function of the first kind of order n. Substituting [2.10] into the right-hand side of [2.8] and writing u_0 in the form

$$u_0 = g(r)(Ce^{-kz} - De^{kz}), \qquad [2.11]$$

Eqs. [2.8] and [2.10] lead to

$$\frac{d^2g}{dr^2} + \frac{1}{r}\frac{dg}{dr} + k^2g = -kJ_0(kr), \quad [2.12]$$

which has as solution

$$g(r) = MJ_0(kr) - \frac{r}{2}J_1(kr), \quad [2.13]$$

where M is a complex constant.

The solution [2.11]–[2.13] of [2.8] yields [2.5] in the form

$$u = 2\dot{h}(t)\left(1 - \frac{r^2}{a^2}\right) + \dot{h}(t)\left(MJ_0(kr) - \frac{r}{2}J_1(kr)\right) \times (Ce^{-kz} - De^{kz}). \quad [2.14]$$

Integrating the continuity Eq. [2.1] gives

$$v = \dot{h}(t)\left(MJ_1(kr) - \frac{r}{2}J_2(kr)\right) \times (Ce^{-kz} + De^{kz}). \quad [2.15]$$

Equations [2.14]–[2.15] satisfy the conditions $\partial u/\partial r = 0$, $v = 0$ at $r = 0$. From the boundary conditions

$$u = v = 0 \quad \text{at} \quad r = a, \quad [2.16]$$

$$M = \frac{a}{2}\frac{J_1(ka)}{J_0(ka)}, \quad [2.17]$$

and

$$J_0(ka)J_2(ka) - J_1^2(ka) = 0. \quad [2.18]$$

This equation has a discrete infinite number of complex roots with positive real and imaginary parts, the first three of which are $k_1a = 4.47 + 1.47i$, $k_2a = 7.69 + 1.73i$, $k_3a = 10.87 + 1.89i$, and, for large n, the asymptotic value is

$$k_na \sim (n + \tfrac{1}{2})\pi + \tfrac{1}{2}i \ln\{(4n + 1)\pi\}. \quad [2.19]$$

The physical pressure p and the velocity components u and v are identified with the real parts of [2.7], [2.14], and [2.15], respectively.

The complete solutions for u and v are infinite sums of the real parts of [2.14] and [2.15], respectively, taken over all the roots k_n ($n = 1, 2, \ldots$). Provided the meniscus has advanced up the tube a distance $z \gg a$, we may neglect the terms proportional to e^{-kz} in [2.14] and [2.15]. It is convenient to introduce the stream function $\psi = \psi(r,z,t)$ where

$$u = -\frac{1}{r}\frac{\partial\psi}{\partial r}, \quad v = \frac{1}{r}\frac{\partial\psi}{\partial z}. \quad [2.20]$$

From [2.14] or [2.15], for $z \gg a$,

$$\psi = \dot{h}(t)\left(\frac{1}{2}\frac{r^4}{a^2} - r^2\right) + \dot{h}(t)\psi_0(r,z),$$

$$\psi_0 = r\sum_n \frac{D_n}{k_n} \times \left(M_nJ_1(k_nr) - \frac{r}{2}J_2(k_nr)\right)e^{k_nz}, \quad [2.21]$$

where M_n is given by [2.17] for $k = k_n$ and the coefficients D_n are determined by applying the boundary conditions at the meniscus.

We wish to examine the assumption that the meniscus has a fixed shape. Let $r' = r$, $z' = z - h(t)$, $\theta' = \theta$ be cylindrical coordinates fixed relative to the meniscus, with corresponding fluid velocity components $v' = v$, $u' = u - \dot{h}(t)$. The intersection of the meniscus with any plane $\theta' = \theta =$ constant must be a stream line in the (r',θ',z') coordinate system, since fluid cannot cross the meniscus and therefore the normal component of the fluid velocity relative to (r',θ',z') vanishes on the meniscus. Thus the stream function ψ' in the (r',θ',z') reference frame is constant on the meniscus. From [2.20] and the corresponding relations in (r',θ',z') coordinates we have

$$\frac{\partial\psi'}{\partial r} = \frac{\partial\psi}{\partial r} + r\dot{h}(t), \quad \frac{\partial\psi'}{\partial z} = \frac{\partial\psi}{\partial z},$$

which, on integrating, gives

$$\psi' = \psi + \tfrac{1}{2}r^2\dot{h}(t) + \text{constant}. \quad [2.22]$$

In particular, on the meniscus ψ' is constant

and therefore, by [2.21]

$$\psi_0 = -\frac{1}{2}\left(\frac{r^4}{a^2} - r^2\right), \qquad [2.23]$$

where an additive constant is equated to zero. Also for the meniscus shape [2.4], the condition that the tangential stress is continuous across the interface is (Appendix I)

$$2\frac{df}{dr}\left(\frac{\partial u}{\partial z} - \frac{\partial v}{\partial r}\right) + \left\{1 - \left(\frac{df}{dr}\right)^2\right\}\left(\frac{\partial u}{\partial r} + \frac{\partial v}{\partial z}\right) = 0. \qquad [2.24]$$

Making use of [2.21] and introducing

$$F_n = D_n e^{k_n h} J_1(k_n a)/k_n, \qquad [2.25]$$

the meniscus condition [2.23] gives

$$\sum_n \frac{F_n r}{J_1(ka)} e^{k_n f(r)}\left\{M_n J_1(k_n r) - \frac{r}{2} J_2(k_n r)\right\} = -\frac{1}{2}\left(\frac{r^4}{a^2} - r^2\right). \qquad [2.26]$$

Forming the sums of [2.14] and [2.15] over all eigenvalues k_n at $z \gg a$, the condition [2.24] gives

$$\sum_n \frac{F_n k_n e^{k_n f(r)}}{J_1(k_n a)}\left[2\frac{df}{dr}\left\{\frac{1}{2} M_n k_n (J_2(k_n r) - 3J_0(k_n r)) + k_n r J_1(k_n r) - \frac{1}{2} J_2(k_n r)\right\} + \left\{1 - \left(\frac{df}{dr}\right)^2\right\}\{(1 + 2k_n M_n) J_1(k_n r) - k_n r J_2(k_n r)\}\right] = \frac{4r}{a^2}\left\{1 - \left(\frac{df}{dr}\right)^2\right\}. \qquad [2.27]$$

The normal stress relation across the meniscus, which determines the shape of the meniscus, is not used. In its place, we assume that the meniscus is a sector of a sphere with a given angle of contact α on the cylindrical wall, so that

$$f(r) = R_c - (R_c^2 - r^2)^{1/2} \qquad [2.28]$$

where $R_c = a \sec \alpha$ is the radius of the sphere. To determine the complex coefficients F_n, we multiply [2.26] and [2.27] by $J_1(j_m r)$ where the j_m $(m = 1, 2, \ldots)$ are the positive roots of $J_1(j) = 0$ and integrate numerically from 0 to a to obtain two infinite sets of equations for the F_n. These equations are truncated and solved for various angles of contact α.

3. THE RATE OF RISE IN A CYLINDRICAL TUBE

To obtain the rate of rise of liquid in the cylindrical tube we integrate the z-component of the Navier–Stokes equations over the volume of the liquid situated in the region bounded by the plane of entry $z = 0$, the wall of the tube $r = a$, and the meniscus given by [2.4] (Fig. 2). Equating the right-hand side of [2.3] to zero in quasi-steady flow, we can write [2.3] as

$$(\nabla \cdot \boldsymbol{\sigma})_z - \rho g = 0, \qquad [3.1]$$

where $\boldsymbol{\sigma}$ is the stress tensor with components in the (r,θ,z) reference frame given by

$$\begin{pmatrix} \sigma_{rr} & 0 & \sigma_{rz} \\ 0 & \sigma_{\theta\theta} & 0 \\ \sigma_{rz} & 0 & \sigma_{zz} \end{pmatrix} = -p\mathbf{U} + \mu \begin{pmatrix} 2\frac{\partial v}{\partial r} & 0 & \frac{\partial v}{\partial z} + \frac{\partial u}{\partial r} \\ 0 & \frac{2v}{r} & 0 \\ \frac{\partial v}{\partial z} + \frac{\partial u}{\partial r} & 0 & 2\frac{\partial u}{\partial z} \end{pmatrix}, \qquad [3.2]$$

where U is the unit tensor of order 3. Integrating [3.1] over the volume of the liquid in the tube and applying the divergence theorem, we obtain the relation of force balance in the z-direction,

$$\int_S \sigma_{zn} dS = \rho g V, \qquad [3.3]$$

where S is the surface bounding V and $\sigma_{zn} = (\boldsymbol{\sigma}\cdot\mathbf{n})_z = \mathbf{k}\cdot\boldsymbol{\sigma}\cdot\mathbf{n}$ the z-component of the vector $\boldsymbol{\sigma}\cdot\mathbf{n}$; $\mathbf{n}$ is the outward unit normal vector to S and $\mathbf{k}$ unit vector in the z-direction. Integrating over the bottom and top and the cylindrical part of S, and dividing by 2π, [3.3] becomes

$$-\int_0^a (\sigma_{zz})_{z=0} r dr + \int_{z=h(t)+f(r)} r\sigma_{zn} ds + a\int_0^{h(t)+f(a)} (\sigma_{zr})_{r=a} dz = \rho g \int_0^a r(h(t) + f(r)) dr. \qquad [3.4]$$

In the second term on the left-hand side, ds is an element of length along a curve on the meniscus which is defined by a constant angle θ.

Using [2.3] and assuming atmospheric pressure p_A at entry to the tube, the first term on the left-hand side of [3.4] becomes

$$\int_0^a p_{z=0} r dr - 2\mu\left[\frac{\partial}{\partial z}\int_0^a r u dr\right] = \tfrac{1}{2}a^2 p_A. \qquad [3.5]$$

Here the second term vanishes because its integral is proportional to the total volume flux in the z-direction and this is independent of z for incompressible flow. If we assume the meniscus to be a sector of a sphere of radius a sec α with angle of contact α, then the normal stress σ_{nn} on the meniscus is given by the condition

$$-\sigma_{nn} = p_A - \frac{2}{a}\gamma_{lg}\cos\alpha \qquad [3.6]$$

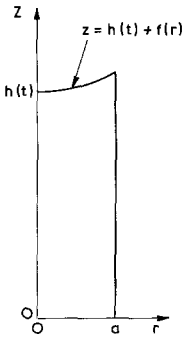

FIG. 2. θ = constant plane section of volume filled with liquid in cylindrical tube.

where γ_{lg} is the liquid/gas interfacial tension. We have used the usual trigonometric relation between meniscus curvature, contact angle, and capillary radius. If we regard α as a macroscopic contact angle and ignore a small correction expressed in terms of line tension (see, for example Pethica (19)), then Young's equation is usually assumed to hold. Thus $\gamma_{lg}\cos\alpha = \gamma_{sg} - \gamma_{sl} = \gamma$, where γ_{sg} and γ_{sl} are, respectively, the solid/gas and solid/liquid interfacial tensions and γ is the adhesion tension. Since the stress on the meniscus has only a normal component, $\sigma_{zn} = \sigma_{nn} n_z$, where n_z is the z-component of unit vector normal to the surface of the meniscus. Hence the second term on the left-hand side of [3.4] becomes

$$\int_{z=h(t)+f(r)} r\sigma_{nn} n_z ds = \left(\frac{2\gamma}{a} - p_A\right)\int_{z=h(t)+f(r)} r n_z ds = \left(\frac{2\gamma}{a} - p_A\right)\frac{a^2}{2}, \qquad [3.7]$$

noting that $n_z ds = dr$.

The third term on the left-hand side of [3.4] requires special attention. We note that $\partial v/\partial z = 0$ at $r = a$ and that the Poiseuille part of u in [2.5] contributes to this third term the expression $-4\mu\dot{h}(t)(h(t) + f(a))$. If the nonslip condition $u = 0$ at $r = a$ is assumed right up to the contact line $z = h(t)$

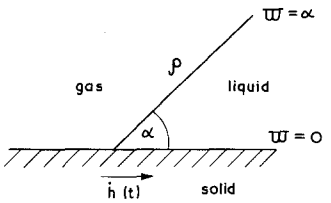

FIG. 3. Region near the three-phase contact line.

$+ f(a)$, then the contribution to the third term from u_0 diverges, as it describes an infinite force acting on the capillary. To avoid this singularity, we terminate the integration with respect to z at a slightly smaller height $h(t) + f(a) - \Delta z$ and now the flow pattern up to this new height corresponds to the outer expansion of Hocking (16) and Huh and Mason (15). Ignoring the term proportional to e^{-kz} in [2.11] and using [2.17],

$$u_0 = \sum_n D_n e^{k_n z}\left\{\frac{r}{2}J_1(k_n r) - \frac{a}{2}\frac{J_1(k_n a)}{J_0(k_n a)}J_0(k_n r)\right\}. \quad [3.8]$$

Hence the outer expansion contributes to the third term in [3.4]

$$\mu a\dot{h}(t)\int_0^{h(t)+f(a)-\Delta z}\left(\frac{\partial u_0}{\partial r}\right)_{r=a}dz = \mu a\dot{h}(t)\int_0^{h(t)+f(a)-\Delta z}\sum_n k_n F_n e^{k_n(z-h(t))}dz = \mu a\dot{h}(t)\sum_n F_n[e^{k_n(f(a)-\Delta z)} - e^{k_n h(t)}]. \quad [3.9]$$

Use has been made of [2.18], [2.25], and standard relations for Bessel functions to obtain the simplified form for $(\partial u_0/\partial r)_{r=a}$ in [3.9]. If we let $\Delta z \to 0$, this series diverges, since, as shown by Hocking (16), it has a singularity of the form

$$\mu a\dot{h}(t)\hat{k}(\alpha)\ln(\Delta z/a),$$

$$\hat{k}(\alpha) = \frac{2(1-\cos 2\alpha)}{2\alpha - \sin 2\alpha}. \quad [3.10]$$

The series [3.9] is truncated, evaluated numerically for $\Delta z > 0$ and [3.10] is subtracted. It was found that, for any particular Δz near to but not equal to zero, this difference fails to converge numerically as more terms are added to the series. The difference at $\Delta z = 0$ is therefore found by extrapolating from values of the difference at somewhat larger Δz where the series does converge numerically. This difference is written as $-\mu a\dot{h}(t)h_0(\alpha)$. Thus for Δz small but different from zero, we have the asymptotic expansion

$$\mu a\dot{h}(t)\int_0^{h(t)+f(a)-\Delta z}\left(\frac{\partial u_0}{\partial r}\right)_{r=a}dz \sim \mu a\dot{h}(t) \times \{\hat{k}(\alpha)\ln(\Delta z/a) - h_0(\alpha)\}. \quad [3.11]$$

The number of terms in the series [3.8] required for an accurate solution depends on the angle of contact, varying from 10 terms for $\alpha = \pi/20$ up to 50 terms for $\alpha = \pi/2$. Consequently the coefficients of the F_n's in equations [2.26] and [2.27] never vary in magnitude so much that rounding errors in the equation-solving routine become significant.

There remains to consider the "inner" expansion in the region $h(t) + f(a) \geqslant z > h(t) + f(a) - \Delta z$ where the nonslip boundary condition is replaced by a suitable slip condition. Since $\Delta z \ll a$ we can approximate to the cylindrical wall of the tube by a plane boundary in the vicinity of the contact line and introduce local polar coordinates ρ, ϖ in the plane of motion with origin on the contact line (Fig. 3). The solid wall and meniscus are defined by $\varpi = 0$ and $\varpi = \alpha$, respectively, and the sector $0 < \varpi < \alpha$ is occupied by the liquid. The meniscus is stationary in this coordinate system. We assume that the velocity of slip of the liquid relative to the wall is proportional to the tangential shear stress. If v_ρ is the velocity of the liquid relative to the wall at the origin, this means that

$$v_\rho - \dot{h}(t) = \frac{c}{\rho}\frac{\partial v_\rho}{\partial \varpi} \quad \text{at} \quad \varpi = 0, \quad [3.12]$$

where c is the slip coefficient, which has

dimensions of length. The inner region where slip of the liquid relative to the wall occurs extends from $\rho = 0$ to $\rho = \Delta z$, where Δz is small compared with the length scale a but large compared with the slip coefficient c. Hocking (16) has shown that this region contributes a force term on the column of liquid in the tube, which, when divided by 2π, equals asymptotically

$$\mu a\dot{h}(t)\{\hat{k}(\alpha) \ln (c/\Delta z) - h_i(\alpha)\}, \quad [3.13]$$

where $h_i(\alpha)$ is obtained by solving numerically an integral equation. Addition of [3.11] and [3.13] removes the force singularity due to the term $\ln \Delta z$. Adding to the sum of [3.11] and [3.13] the corresponding Poiseuille term $-4\mu\dot{h}(t)(h(t) + f(a))$ and multiplying by -2π, we obtain the force on length $h(t) + f(a)$ of the tube in contact with the liquid due to the viscous drag, namely,

$$F = 8\pi\mu\dot{h}(t)[h(t) + f(a) + ae], \quad [3.14]$$

where

$$e = \tfrac{1}{4}[\hat{k}(\alpha) \ln (a/c) + h_i(\alpha) + h_0(\alpha)] \quad [3.15]$$

Any deviation from Poiseuille flow near the tube entrance has been neglected here.

The integrals on the left-hand side of [3.4] are now determined and substitution of [2.28] for $f(r)$ yields the right-hand side of [3.4]. It follows that [3.4] gives

$$\dot{h}(t) = \frac{(a\gamma - \rho g V')}{4\mu[h(t) + f(a) + ae]}, \quad [3.16]$$

where

$$V' = \frac{V}{2\pi} = \tfrac{1}{2}h(t)a^2 + \tfrac{1}{3}a^3(\sec^3 \alpha - \tan^3 \alpha). \quad [3.17]$$

Equation [3.16] is a generalization of Washburn's formula for the rate of rise of liquid up a cylindrical tube. The condition that the pressure at the capillary entrance is atmospheric can be removed by assuming that the fluid velocity in the reservoir describes a sink flow toward entry into the capillary. According to Levine *et al.* (7), e is replaced by $e + \frac{1}{4}$ in [3.16]. Washburn's equation is obtained from [3.16] by putting $f(a) = 0$ and $e = 0$. We see that the extra drag due to the meniscus increases the effective height $h(t)$ by an amount $f(a) + ae$, which can exceed considerably the corresponding entry correction.

In discussing the meaning of the slip coefficient c, Hocking (20) introduces three length scales, macroscopic, microscopic, and molecular, where the microscopic length measures the surface irregularities of the solid wall. Assuming that the nonslip condition holds on the microscopic length scale at the boundary of the fluid with the solid wall, Hocking shows that a fictitious smooth surface through the "crests" of the irregularities can be drawn such that at macroscopic distances from the boundary the fluid flow is reproduced with an equivalent slip condition at this fictitious surface. In other words, a shear stress proportional to the slip velocity at this surface gives the same fluid flow as the nonslip condition on the solid boundary at macroscopic distances from this boundary. The conclusion (20, 21) is that in ordinary single phase flow past a solid boundary which involves no infinite stresses, the size of the slip coefficient (zero in the absence of slip) can be ignored and so the usual condition of nonslip is satisfactory in regard to the predictions of the macroscopic fluid flow. However, in those special cases where the nonslip condition predicts an infinite stress, then the magnitude of the slip coefficient becomes important and such a special situation is found at the three-phase contact line in two-phase flow.

If we follow Hocking (20) and identify the slip coefficient c with that due to the microscopic surface irregularities, then two limiting values of c can be considered: (i) For shallow irregularities, c is proportional to (roughly half) the mean depth of the irregularities, and (ii) for deep irregularities c is proportional to (roughly one-tenth) the

mean separation between successive crests. We choose two values of c, 10^{-4} cm which is a typical measure and 10^{-6} cm, which is the lower limit of the microscopic irregularities.

Huh and Mason (15) are concerned with removing the mathematical singularity arising from the continuum formulation of the fluid dynamic problem of the moving three-phase contact line with the nonslip condition. They choose what they regard is a lower bound on c, namely, the diameter of a molecule ($\frac{1}{2} \times 10^{-7}$ cm). Their c is a slip coefficient on the molecular scale, giving the largest possible deviation from the classical Washburn equation. Huh and Mason (15) refer to an approximate theory by Tolstoi (22) which predicts values of c/a (on the molecular scale) in terms of molecular parameters of the fluid in question. Tolstoi assumes a slip mechanism similar to that in the treatment of electrical conductivity of ionic crystals (23). This mechanism is also used in a theory of slip velocity on a molecular scale by Ruckenstein and Dunn (24). These authors postulate that slip occurs because of a gradient in the chemical potential of the liquid molecules in the neighborhood of the contact line between the three phases solid/liquid/gas. However, their result is not expressed in the form [3.12] with a slip coefficient c.

A mathematically identical slip-flow boundary condition to [3.12] (i.e., slip-flow proportional to surface shear stress) was postulated and experimentally verified by Beavers and Joseph (25) to resolve difficulties which arise in the related problem of fluid flow past a porous surface. In such situations the Darcy equation is solved within the porous medium and the Navier–Stokes equation outside the medium, with the slip-flow boundary condition matching the two solutions at the interface. Subsequently Taylor (26) and Richardson (27) confirmed the slip-flow boundary condition of Beavers and Joseph experimentally and theoretically for a parallel plate-channel model of the porous medium. Also, Saffman (28) derived the slip-flow condition from statistical considerations. In the case of the porous surface problem the slip coefficient, c, is equal to $K^{1/2}/\beta$ where K denotes the permeability of the medium (being a direct measure of the square of the mean pore size) and β is a dimensionless constant of order 1 which characterizes the internal surface and structure of the medium (25–29). Flow past a porous medium and a solid surface exhibiting roughness and heterogeneity should have similarities if the wall region of the surface may be approximated by a porous layer of microscopic thickness. Since c is of the same order as the mean pore size, in the porous surface model, by analogy it would be of the same order as the dimensions of the surface roughness. Such a value of c obviously refers to the microscopic length scale of Hocking (20). The experimental results of

TABLE I

Values of $\hat{k}(\alpha)$, $h_i(\alpha)$ and $h_0(\alpha)$.

α/π	$\hat{k}(\alpha)$	$h_i(\alpha)$	Cylindrical tube $h_0(\alpha)$	Parallel-plate channel $h_0(\alpha)$
0.05	19.04	−56.3	−30.4	−29.4
0.1	9.42	−21.6	−12.7	−11.5
0.2	4.52	−7.42	−5.88	−5.10
0.25	3.50	−4.33	−4.76	−4.10
0.5[a]	1.27	−0.148	−2.27	−2.02

[a] The incorrect value $h_i(\alpha) + h_0(\alpha) = -1.90$ at $\alpha/\pi = 0.5$ for the cylindrical tube is quoted by Hocking (16). Our results agree with those of Huh and Mason (15).

TABLE II

Values of e (Cylindrical Tube)

	c/a				
α/π	10^{-2}	10^{-3}	10^{-4}	10^{-5}	10^{-6}
0.05	0.23	11.18	22.14	33.10	44.06
0.1	2.28	7.70	13.13	18.55	23.97
0.2	1.88	4.49	7.09	9.69	12.30
0.25	1.76	3.78	5.79	7.81	9.83
0.5	0.86	1.59	2.33	3.06	3.79

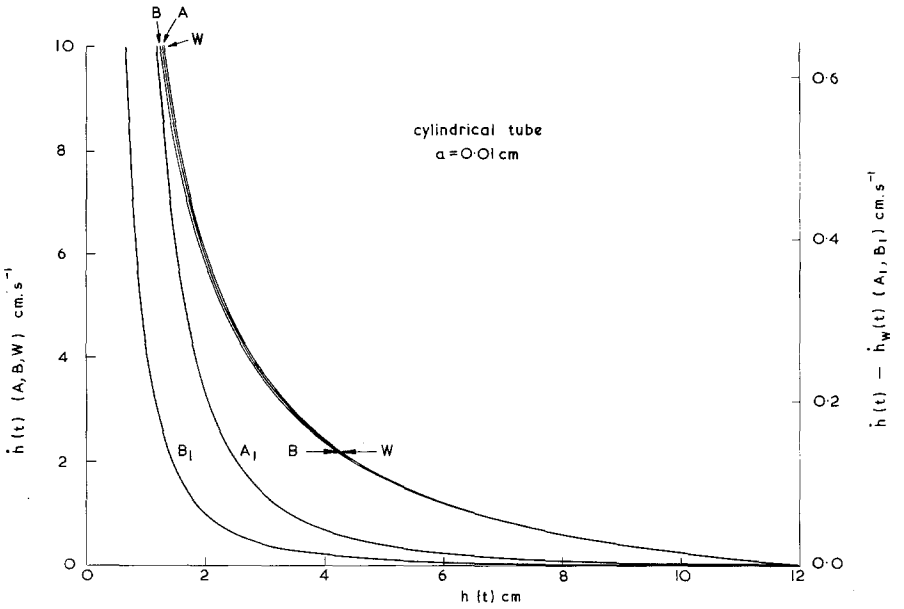

FIG. 4. Plots of rate of capillary rise (cm sec^{-1}) against meniscus height $h(t)$ (cm) in a cylindrical tube of radius $a = 0.01$ cm at two values of the slip coefficient c. For curves A and A_1, $c = 10^{-4}$ cm and for curves B and B_1, $c = 10^{-6}$ cm. Left-hand vertical axis gives velocity $\dot{h}(t)$ for curves A and B and $\dot{h}_W(t)$ for the Washburn equation. Right-hand axis gives velocity difference $\dot{h}(t) - \dot{h}_W(t)$ for curves A_1 and B_1.

Beavers and Joseph (25) and of Taylor (26) on flow past porous media seem quite consistent with the slip condition [3.12] used in this paper.

Table I gives values of $\hat{k}(\alpha)$ and $h_i(\alpha)$ as calculated by Hocking (16), and values of $h_0(\alpha)$ determined in this paper, for different contact angles α.

Table II gives values of e for different ratios c/a and contact angles α. From Table II, it is seen that e, which is a measure of the increase in viscous drag due to the presence of the meniscus, increases with decreasing contact angle, for the smaller values of c/a. Indeed, as α approaches zero, we have the physically unrealistic situation of e becoming very large. However, the approximate theory proposed by Tolstoi (22) to predict values of c/a in terms of molecular parameters suggests that c is very sensitive to α with $a/c = 0$ when $\alpha = 0$. It is therefore probable that a decrease in α should be accompanied by a corresponding increase in c/a if one is to relate the corresponding values of e. The fact that the column $c/a = 10^{-2}$ in Table II does not follow strictly the pattern of increasing e with decreasing α described above probably arises because e is the difference between two nearly equal large numbers for the angles $\alpha/\pi = 0.05$ and 0.1. Thus, only a small error in either of these numbers can lead to a large error in e.

Figure 4 shows plots of $\dot{h}(t)$ obtained from Eq. [3.16] and from the Washburn equation and also the corresponding difference in $\dot{h}(t)$ against $h(t)$ for $a = 0.01$ cm. Figure 5 gives $\dot{h}(t)$ against $h(t)$ for $a = 0.1$ cm. Values of other relevant physical quantities are $\rho = 1$ g cm^{-3}, $\mu = 0.01$ P, $\gamma_{lg} = 72$ dyn cm^{-1}, $\alpha = \pi/5$, and two values of the slip coefficient $c = 10^{-4}$ and 10^{-6} cm, representing, respectively, slip due to tube wall microscopic irregularities and to surface properties on a molecular length scale. It is seen that for $a = 0.01$ cm the deviation from the Washburn equation is small, being the greater for slip on a molec-

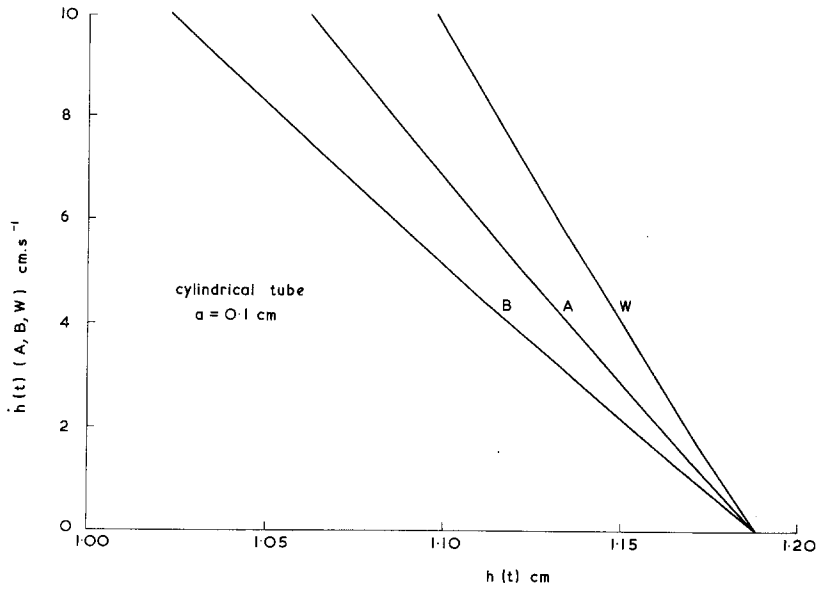

FIG. 5. Plots of $h(t)$ (cm sec^{-1}) against $h(t)$ (cm) in cylindrical tube of radius $a = 0.1$ cm. Curve W, Washburn; curve A, $c = 10^{-4}$ cm; curve B, $c = 10^{-6}$ cm.

ular length scale. However, for the wider tube of radius $a = 0.1$ cm, the deviation from the Washburn equation can be appreciable. Of course, the different $\dot{h}(t) - h(t)$ curves join at the equilibrium position of the meniscus, where $\dot{h}(t) = 0$.

Equation [3.16] can be integrated to yield the height $h(t)$ as a function of time t in the form

$$\ln\left(1 - \frac{h}{h_{eqm}}\right)^{-1} - \frac{h}{[h_{eqm} + f(a) + e]} = \left(\frac{\rho g a^2}{8\mu}\right)\frac{t}{[h_{eqm} + f(a) + ae]} + \beta \quad [3.18]$$

where β is a constant of integration and h_{eqm} is the equilibrium height defined by $\dot{h}(t) = 0$. According to [3.16]

$$h_{eqm} = \frac{2\gamma}{\rho g a} - \frac{2}{3}a(\sec^3\alpha - \tan^3\alpha). \quad [3.19]$$

The Lucas–Washburn (L.W.) equation is obtained by putting $f(a) = 0$ and $e = 0$. If it is assumed that $h(t) = 0$ at $t = 0$, then $\beta = 0$ and if further, we expand in powers of h/h_{eqm}, then for small values of this ratio,

$$(h/h_{eqm})^2 = \frac{\rho g a^2}{4\mu h_{eqm}} t \quad [3.20]$$

a result which is quoted in the literature. However it should be stressed that equation [3.16] does not hold near $t = 0$. According to Szekely *et al.* (8), Levine *et al.* (7), and Levine and Neale (30), acceleration and nonlinear dissipation effects must be considered at the initial stages of entry of the liquid into the tube from the reservoir. Fortunately these effects die off at distances up the tube of the order of a tube diameter, and the quasi-steady flow assumed here is reached in a very short time (a matter of about 10^{-3} sec for $a = 0.01$ cm). The constant β therefore corresponds to a time interval of this magnitude. In the above discussion we have not taken into account the effect of introducing the values of $f(a)$ and e. Blake *et al.* (31) tested experimentally the L.W. equation ($f(a) = 0$ and $e = 0$ in [3.18]) and found an increasing divergence from the L.W. equation as equilibrium was reached.

4. RATE OF RISE OF MENISCUS UP A PARALLEL-PLATE CHANNEL

We introduce Cartesian coordinates (x,y,z) and corresponding fluid velocity components $(0,v,w)$. z is the vertical axis upward and x and y horizontal axes parallel and normal, respectively, to the two plates, with origin on the median plane at the entrance to the channel. Flow conditions are taken independent of x so that the velocity components v and w, together with the pressure p, are functions of y, z, and the time t. The area of the two plates, at separation $2a$, is assumed infinite. For two-dimensional incompressible flow the equation of continuity is

$$\frac{\partial v}{\partial y} + \frac{\partial w}{\partial z} = 0, \qquad [4.1]$$

and the Navier–Stokes equations are

$$\frac{\partial v}{\partial t} + v\frac{\partial v}{\partial y} + w\frac{\partial v}{\partial z} = -\frac{1}{\rho}\frac{\partial p}{\partial y} + \frac{\mu}{\rho}\left(\frac{\partial^2 v}{\partial y^2} + \frac{\partial^2 v}{\partial z^2}\right), \qquad [4.2]$$

$$\frac{\partial w}{\partial t} + v\frac{\partial w}{\partial y} + w\frac{\partial w}{\partial z} = -\frac{1}{\rho}\frac{\partial p}{\partial z} + \frac{\mu}{\rho}\left(\frac{\partial^2 w}{\partial y^2} + \frac{\partial^2 w}{\partial z^2}\right). \qquad [4.3]$$

Similarly to the cylindrical case, we consider the quasi-steady-state flow for which the meniscus is assumed to have a fixed shape, specified at time t by

$$z = h(t) + f(y), \qquad [4.4]$$

where $h(t)$ is the meniscus height on the median plane. We assume the left-hand sides of [4.2] and [4.3] to be zero and seek solutions of the form

$$w = \frac{3}{2}\dot{h}(t)\left(1 - \frac{y^2}{a^2}\right) + \dot{h}(t)w_0(y,z), \qquad [4.5]$$

$$v = \dot{h}(t)v_0(y,z), \qquad [4.6]$$

$$p = -\left(\rho g + \frac{3}{a^2}\mu\dot{h}(t)\right)z + \dot{h}(t)p_0(y,z), \qquad [4.7]$$

where the first terms in w and p describe Poiseuille flow. $p_0(y,z)$ satisfies Laplace's equation, for which a particular solution in the vicinity of the meniscus is

$$p_0(y,z) = \mu(A \sin ky + B \cos ky)e^{kz}, \qquad [4.8]$$

where A, B, and k are constants and we assume $z \gg a$. The equation satisfied by w_0 is

$$\frac{\partial^2 w_0}{\partial y^2} + \frac{\partial^2 w_0}{\partial z^2} = \frac{1}{\mu}\frac{\partial p_0}{\partial z}. \qquad [4.9]$$

On substituting [4.8] for p_0 and writing w_0 in the form $e^{kz}g(y)$ a solution for $g(y)$ is readily found. The nondimensional velocity components v_0, w_0 are related by the continuity equation [4.1], which on integration gives v_0. On applying the symmetry conditions

$$\frac{\partial w_0}{\partial y} = 0, \quad v_0 = 0 \quad \text{at} \quad y = 0, \qquad [4.10]$$

we find that $A = 0$ and

$$w_0 = e^{kz}[-Q \cos ky + \tfrac{1}{2}By \sin ky], \qquad [4.11]$$

$$v_0 = e^{kz}\left[\left(Q - \frac{B}{2k}\right) \times \sin ky + \tfrac{1}{2}By \cos ky\right], \qquad [4.12]$$

which depend on constants Q and B. The boundary conditions

$$w_0 = 0, \quad v_0 = 0 \quad \text{at} \quad y = a \qquad [4.13]$$

yield

$$Q = \tfrac{1}{2}Ba \tan ka, \qquad [4.14]$$

$$\sin 2ka = 2ka. \qquad [4.15]$$

Similarly to [2.18], Eq. [4.15] has a discrete infinite number of complex roots k_n ($n = 1, 2, \ldots$) with positive real and imaginary parts. The asymptotic form of k_n differs from [2.19] only in that the real part of $k_n a$ equals $(n + \tfrac{1}{4})\pi$. Summing over the

roots of [4.15], we obtain

$$w_0 = \tfrac{1}{2} \sum_n B_n e^{k_n z} \times [-a \tan k_n a \cos k_n y + y \sin k_n y], \quad [4.16]$$

$$v_0 = \tfrac{1}{2} \sum_n B_n e^{k_n z} \times [-a \cot k_n a \sin k_n y + y \cos k_n y]. \quad [4.17]$$

The (complex) coefficients B_n are determined by applying the boundary conditions at the meniscus.

The stream function is

$$\psi = \frac{3}{2}\dot{h}(t)\left(y - \frac{1}{3}\frac{y^3}{a^2}\right) + \dot{h}(t)\psi_0(y,z), \quad [4.18]$$

where ψ_0 is due to the deviation from Poiseuille flow. Integration of the relation $v_0 = -\partial\psi_0/\partial z$ yields

$$\psi_0 = \frac{1}{2}\sum_n \frac{B_n}{k_n} e^{k_n z} \times (a \cot k_n a \sin k_n y - y \cos k_n y). \quad [4.19]$$

TABLE III

Values of e (Parallel-Plate Channel)

	c/a				
α/π	10^{-2}	10^{-3}	10^{-4}	10^{-5}	10^{-6}
0.05	0.66	15.27	29.88	44.49	59.10
0.1	3.45	10.68	17.91	25.14	32.38
0.2	2.77	6.24	9.71	13.18	16.65
0.25	2.57	5.26	7.95	10.63	13.32
0.5	1.23	2.21	3.19	4.16	5.14

By an argument similar to that used to derive [2.23] the condition that the meniscus has a fixed shape yields

$$\psi_0 = \frac{1}{2}\left(\frac{y^3}{a^2} - y\right) \quad [4.20]$$

on the meniscus. Writing

$$F_n = \frac{1}{2}\frac{B_n}{k_n} \sin k_n a \, e^{k_n h(t)}, \quad [4.21]$$

equating [4.19] to [4.20] on the meniscus and using [4.4], we obtain

$$\sum_n F_n \frac{e^{k_n f(y)}}{\sin^2 k_n a}(a \cos k_n a \sin k_n y - y \cos k_n y \sin k_n a) = \frac{1}{2}\left(\frac{y^3}{a^2} - y\right). \quad [4.22]$$

The condition of zero tangential stress at the meniscus is

$$2\frac{df}{dy}\left(\frac{\partial w}{\partial z} - \frac{\partial v}{\partial y}\right) + \left(1 - \left(\frac{df}{dy}\right)^2\right)\left(\frac{\partial w}{\partial y} + \frac{\partial v}{\partial z}\right) = 0. \quad [4.23]$$

Making use of [4.5], [4.6], [4.16], and [4.17] this yields

$$\sum_n k_n F_n e^{k_n f(y)}\left[-2\frac{df}{dy}(a \sin k_n a \cos k_n y - y \sin k_n y \cos k_n a) + \left(1 - \left(\frac{df}{dy}\right)^2\right)(a \sin k_n a \sin k_n y + y \cos k_n y \cos k_n a)\right] = \frac{3y}{2a}\left(1 - \left(\frac{df}{dy}\right)^2\right). \quad [4.24]$$

We shall assume that the meniscus is a section of a circular cylinder with an angle of contact α at the two plates. Then

$$f(y) = R_c - (R_c^2 - y^2)^{1/2} \quad [4.25]$$

where $R_c = a \sec \alpha$ is the radius of the circle. To determine the coefficients F_n we multiply [4.22] and [4.24] by $\sin(m\pi y/a)$ ($m = 1, 2, \ldots$) and numerically integrate from 0 to a. The two infinite sets of equations for F_n were truncated and solved for different α, and B_n is determined from [4.21]. As in the cylindrical case, the real parts of the series [4.16] and [4.17] describe the physical velocity components.

The treatment of the rate of rise of liquid

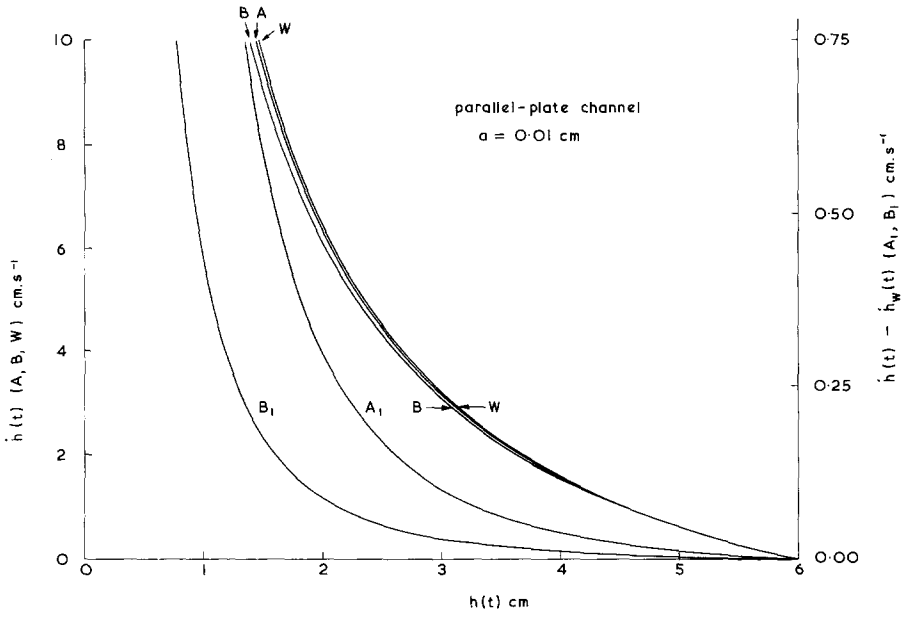

FIG. 6. Plots corresponding to those in Fig. 4 for flow in parallel-plate channel at half-separation $a = 0.01$ cm and $c = 10^{-4}$ cm (curves A, A_1) and $c = 10^{-6}$ cm (curves B, B_1).

in the parallel-plate channel is similar to that in Section 3. We integrate the z-component of the Navier–Stokes equations over the volume of liquid per unit width of the infinite plates, bounded by $z = 0$, the median plane $y = 0$, the plate $y = a$, and the meniscus given by [4.4]. Noting that the shear stress is zero on the median plane, Eq. [3.4] is replaced by

$$-\int_0^a (\sigma_{zz})_{z=0}dy + \int_{z=h(t)+f(y)} \sigma_{zn}ds + \int_0^{h+f(a)} (\sigma_{yz})_{y=a}dz = \rho g \int_0^a (h(t) + f(y))dy. \quad [4.26]$$

If we assume atmospheric pressure p_A at entry to the parallel plate channel and use Laplace's equation at the meniscus, then the sum of the first two terms in [4.26] equals γ. The outer expansion contributes to the third term

$$\mu\dot{h}(t)\int_0^{h(t)+f(a)-\Delta z}\left(\frac{\partial w_0}{\partial y}\right)_{y=a}dz = -\mu\dot{h}(t)\int_0^{h(t)+f(a)-\Delta z}\sum_{n=1}^{\infty} B_n \sin k_n a\, e^{k_n z}dz$$

$$= -2\mu\dot{h}(t)\sum_{n=1}^{\infty} F_n[e^{k_n(f(a)-\Delta z)} - e^{k_n h(t)}], \quad [4.27]$$

which has the asymptotic form as $\Delta z \to 0$

$$\mu\dot{h}(t)[\hat{k}(\alpha)\ln(\Delta z/a) - h_0(\alpha)]. \quad [4.28]$$

The inner expansion contributes to the third term

$$\mu\dot{h}(t)\{\hat{k}(\alpha)\ln(c/\Delta z) - h_i(\alpha)\}. \quad [4.29]$$

Finally substituting [4.25] for $f(y)$, the right-hand side of [4.26] equals

$$\rho g A' = \rho g\left[h(t)a + R_c a - \frac{1}{2}R_c^2\left\{\sin^{-1}\left(\frac{a}{R_c}\right) + \frac{a}{R_c}\left(1 - \frac{a^2}{R_c^2}\right)^{1/2}\right\}\right] \quad [4.30]$$

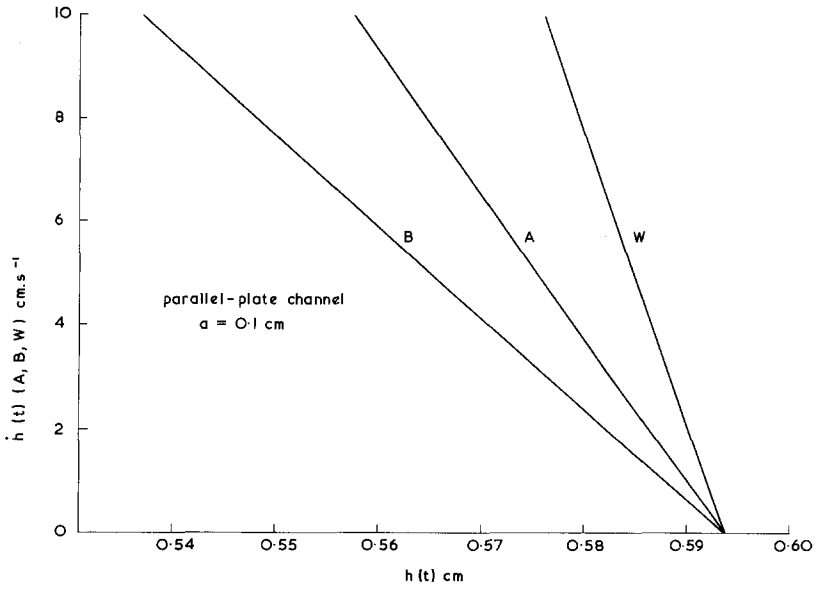

FIG. 7. Plots corresponding to those in Fig. 5 for flow in parallel-plate channel at half-separation $a = 0.1$ cm and $c = 10^{-4}$ cm (curve A) and $c = 10^{-6}$ cm (curve B).

where A' is the area of cross-section of liquid between a plate and the median plane in the yz plane. The relation [4.26] therefore yields

$$\dot{h}(t) = \frac{a(\gamma - \rho g A')}{3\mu[h(t) + f(a) + ae]} . \quad [4.31]$$

The plane Washburn equation is obtained by putting $e = 0$.

Table I applies to both the cylindrical tube and parallel-plate channel, since on the length scale Δz of the inner region the cylindrical tube is virtually plane. Table III gives values of e for the parallel-plate channel. The values of e are somewhat greater than their counterparts in Table II for a cylindrical tube. Figures 6 and 7 show plots of $\dot{h}(t)$ against $h(t)$ which correspond to those in Figs. 4 and 5.

APPENDIX I

Let **n** and **t** denote unit vectors normal and tangential, respectively, to a curve on the meniscus which is defined by θ = constant. If the shape of the meniscus is given by [2.4], then in (r,θ,z) coordinates,

$$\mathbf{n} = \frac{\left(-\frac{df}{dr}, 0, 1\right)}{\left[1 + \left(\frac{df}{dr}\right)^2\right]^{1/2}},$$

$$\mathbf{t} = \frac{\left(1, 0, \frac{df}{dr}\right)}{\left[1 + \left(\frac{df}{dr}\right)^2\right]^{1/2}}.$$

The condition for zero tangential stress at the meniscus is

$$0 = \sigma_{nt} = \mathbf{n}\cdot\boldsymbol{\sigma}\cdot\mathbf{t}$$

$$= \frac{1}{\left[1 + \left(\frac{df}{dr}\right)^2\right]^{1/2}}\left(-\frac{df}{dr}, 0, 1\right) \times \begin{pmatrix} \sigma_{rr} & 0 & \sigma_{rz} \\ 0 & \sigma_{\theta\theta} & 0 \\ \sigma_{rz} & 0 & \sigma_{zz} \end{pmatrix} \begin{pmatrix} 1 \\ 0 \\ \frac{df}{dr} \end{pmatrix}.$$

On substituting [3.2], the relation [2.24] readily follows. In a similar manner, we easily derive [4.23].

ACKNOWLEDGMENTS

We are indebted to Tioxide International Limited and to the Science Research Council of the United Kingdom, for a postdoctoral research assistantship to J.L.

REFERENCES

1. Wingrave, J. A., Wade, W. H., and Schechter, R. S. *in* "Wetting, Spreading and Adhesion," S.C.I. Symposium, Sept. 1976, Loughborough (J. F. Padday, Ed.), pp. 261–288. Academic Press, London, 1978.
2. Lucas, R., *Kolloid-Z.* **23,** 15 (1918).
3. Bosanquet, C. H., *Phil. Mag.* (Ser. 6) **45,** 525 (1923).
4. Washburn, F. W., *Phys. Rev.* **17,** 273 (1921).
5. Rideal, E. K., *Phil. Mag.* (Ser. 6) **44,** 1152 (1922).
6. Levine, S., and Neale, G., *Faraday Trans. II* **71,** 12 (1975).
7. Levine, S., Reed, P., Watson, E. J., and Neale, G., *in* "Colloid and Interface Science" (M. Kerker, Ed.), Vol. III, p. 403. Academic Press, New York, 1976.
8. Szekely, J., Neumann, A. W., and Chuang, Y. K., *J. Colloid Interface Sci.* **35,** 273 (1971).
9. Huh, C., and Scriven, L. E., *J. Colloid Interface Sci.* **35,** 85 (1971).
10. van Dussan, E. B., and Davies, S. H., *J. Fluid Mech.* **65,** 71 (1974).
11. Van Dyke, M., "Perturbation Methods in Fluid Mechanics." Academic Press, New York, 1964.
12. van Dussan, E. B., *J. Fluid Mech.* **77,** 665 (1976).
13. Bataille, M., *C. R. Acad. Sci. Paris* **262,** 843 (1966).
14. Bhattacharji, S., and Savic, P., *Proc. Heat Transfer. Fluid Mech. Inst.* **1965,** 248.
15. Huh, C., and Mason, S. G., *J. Fluid Mech.* **81,** 401 (1977).
16. Hocking, L. M., *J. Fluid Mech.* **79,** 209 (1977).
17. Hansen, R. J., and Toong, T. Y., *J. Colloid Interface Sci.* **37,** 196 (1971).
18. Hansen, R. J., and Toong, T. Y., *J. Colloid Interface Sci.* **36,** 410 (1971).
19. Pethica, B. A., *J. Colloid Interface Sci.* **62,** 567 (1977).
20. Hocking, L. M., *J. Fluid Mech.* **76,** 801 (1976).
21. Richardson, S., *J. Fluid Mech.* **59,** 707 (1973).
22. Tolstoi, D. M., *Dokl. Akad. Nauk SSSR* **85,** 1089 (1952).
23. Frenkel, J., "Kinetic Theory of Liquids." Oxford Univ. Press, London/New York, 1946.
24. Ruckenstein, E., and Dunn, C. S., *J. Colloid Interface Sci.* **59,** 135 (1977).
25. Beavers, G. S., and Joseph, D. D., *J. Fluid Mech.* **30,** 197 (1967).
26. Taylor, G. I., *J. Fluid Mech.* **49,** 319 (1971).
27. Richardson, S., *J. Fluid Mech.* **49,** 327 (1971).
28. Saffman, P. G., *Studies Appl. Math.* **50,** 93 (1971).
29. Neale, G., and Nader, W., *Canad. J. Chem. Eng.* **52,** 475 (1974).
30. Levine, S., and Neale, G., *in* "Wetting, Spreading and Adhesion," S.C.I. Symposium, Sept. 1976, Loughborough (J. F. Padday, Ed.), pp. 241–260. Academic Press, London, 1978.
31. Blake, T. D., Everett, D. H., and Haynes, J. M., *Wetting, S.C.I. Monograph* **25,** 164 (1967).